Advances in Nano Research, *Vol. 15, No. 5 (2023) 451-466*
https://doi.org/10.12989/anr.2023.15.5.451

Nanotechnology in early diagnosis of gastro intestinal cancer surgery through CNN and ANN-extreme gradient boosting

Y. Wenjing*[1†], T. Yuhan[1†], Y. Zhiang[1], T. Shanhui[1], L. Shijun[1], M. Sharaf[2]

[1]*Institute of Life Science, Wenzhou University, Wenzhou, China*
[2]*Industrial Engineering Department, College of Engineering, King Saud University, P.O. Box 800, Riyadh 11421, Saudi Arabia*

(*Received February 1, 2022, Revised July 10, 2023, Accepted July 11, 2023*)

Abstract. Gastrointestinal cancer (GC) is a prevalent malignant tumor of the digestive system that poses a severe health risk to humans. Due to the specific organ structure of the gastrointestinal system, both endoscopic and MRI diagnoses of GIC have limited sensitivity. The primary factors influencing curative efficacy in GIC patients are drug inefficacy and high recurrence rates in surgical and pharmacological therapy. Due to its unique optical features, good biocompatibility, surface effects, and small size effects, nanotechnology is a developing and advanced area of study for the detection and treatment of cancer. Because of its deep location and complex surgery, diagnosing and treating gastrointestinal cancer is very difficult. The early diagnosis and urgent treatment of gastrointestinal illness are enabled by nanotechnology. As diagnostic and therapeutic tools, nanoparticles directly target tumor cells, allowing their detection and removal. XGBoost was used as a classification method known for achieving numerous winning solutions in data analysis competitions, to capture nonlinear relations among many input variables and outcomes using the boosting approach to machine learning. The research sample included 300 GC patients, comprising 190 males (72.2% of the sample) and 110 women (27.8%). Using convolutional neural networks (CNN) and artificial neural networks (ANN)-EXtreme Gradient Boosting (XGBoost), the patients mean± SD age was 50.42 ± 13.06. High-risk behaviors (P = 0.070), age at diagnosis (P = 0.037), distant metastasis (P = 0.004), and tumor stage (P = 0.015) were shown to have a statistically significant link with GC patient survival. AUC was 0.92, sensitivity was 81.5%, specificity was 90.5%, and accuracy was 84.7 when analyzing stomach picture.

Keywords: artificial neural networks; convolutional neural networks; extreme gradient boosting; gastrointestinal cancer; nanotechnology

1. Introduction

Timely identification of gastric cancer is a crucial determinant in enhancing the overall outcomes of patients. The detection rate of gastric cancer exhibits variations based on the level of experience of the endoscopist (Zhang *et al*. 2015). Over the past decade, deep-learning-based machine learning techniques have demonstrated noteworthy advancements in image recognition, leading to their application in diverse medical domains (Esteva *et al*. 2017, Shichijo *et al*. 2017, Horie *et al*. 2019, Song *et al*. 2023, Lu *et al*. 2023, Dang *et al*. 2023). The effectiveness of the convolutional neural network (CNN) system, based on deep learning, in detecting gastric cancer in static images was presented. A detection rate of 92.2% overall and 98.6% for diameters greater than 6 mm was demonstrated by the CNN system. Additionally, a high processing speed of 2296 images per 47 seconds was exhibited by it (Hirasawa *et al*. 2018). These results suggest that the CNN system has the potential to assist endoscopists in improving diagnostic yields. In order to implement this technology for the prompt identification of gastric cancer during routine screening esophagogastroduodenoscopy, we carried out a preliminary investigation to assess the efficacy of our Convolutional Neural Network (CNN) system when applied to video images. (Lu *et al*. 2023, Zhu *et al*. 2021, Zhuang *et al*. 2022) A total of 68 endoscopic submucosal dissection procedures were performed on 62 patients with early gastric cancer, and video images were obtained for analysis (refer to Table S1). The objective of the study was to evaluate the accuracy of our CNN system in detecting lesions, as demonstrated in Fig. 1. The findings indicate that the CNN accurately identified 94.1% of the total 68 lesions, correctly diagnosing 64 of them. Our findings for static images align with this statement. The median time for lesion detection was 1 second, with a range of 0 to 44 seconds, measured from the moment the lesions initially appeared on the screen. Gastric Gastrointestinal Stromal Tumor is shown in Fig. 1.

Enhancing the precision of endoscopic diagnostics for early-stage gastric cancer and precancerous lesions would significantly aid in mitigating the occurrence and fatality of gastric cancer. In addition, early detection of lesions prior to their progression into invasive cancer can facilitate their removal through endoscopic resection, resulting in a noteworthy enhancement of the patients' health-related quality of life (Fujishiro *et al*. 2017). Hence, it is crucial to strive toward enhancing the diagnostic precision of gastric mucosal lesions to prevent and treat gastric cancer effectively. The technique of magnifying endoscopy with

*Corresponding author, Ph.D., Professor
E-mail: ynagwenjing@hotmail.com
† These authors contributed equally to this work

Copyright © 2023 Techno-Press, Ltd.

ISSN: 2287-237X (Print), 2287-2388 (Online)

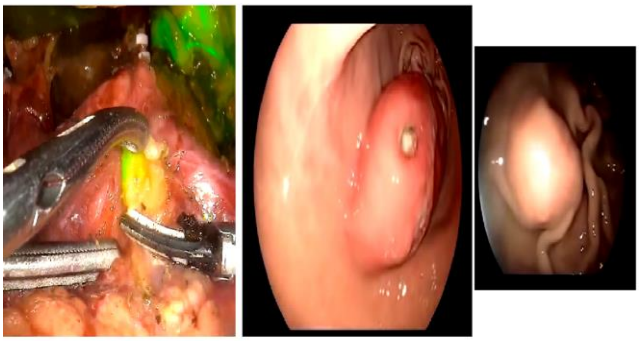

Fig. 1 Gastric gastrointestinal stromal tumor

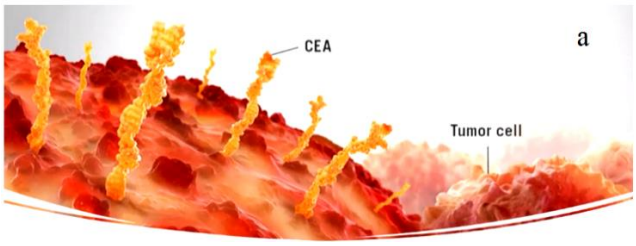

Fig. 2 Schematic view carcinoembryonic antigen CEA

narrow band imaging (M-NBI) has been employed to investigate the glandular epithelium of the stomach by analyzing the microvascular architecture and microsurface structure. This method has been found to have a significantly higher level of accuracy compared to conventional white light endoscopes, as reported in several studies (Kaise *et al*. 2009, Pimentel-Nunes *et al*. 2012, Yao 2015). According to expert recommendations, the use of an algorithm known as magnifying endoscopy simple diagnostic algorithm for early gastric cancer (MESDA-G) is advisable for the purpose of distinguishing between non-cancerous lesions and early gastric cancers (Muto *et al*. 2016). Multiple studies have reported that the sensitivity of M-NBI in detecting early gastric cancer ranges from 85.7% to 97.3%, and the specificity ranges from 84.4% to 96.8%, based on the algorithm used. These findings are supported by references 11-13. The diagnostic accuracy of individuals without specialized expertise in distinguishing between early gastric cancer and non-cancerous lesions using M-NBI was generally unsatisfactory, as reported in previous studies (Kadowaki *et al*. 2009, Shibagaki *et al*. 2015, White *et al*. 2018). In order to address the limitations of traditional medical diagnosis methods, the implementation of artificial intelligence has been proposed as a potential solution (Das *et al*. 2018, Li *et al*. 2019). Currently, deep learning has successfully overcome the limitations of traditional machine learning in the field of artificial intelligence. This has led to improved performance in medical tasks such as image classification, and has opened up new avenues for exploring the application of artificial intelligence in medical practice (Chartrand *et al*. 2017, Abdelhafiz *et al*. 2019, He *et al*. 2020). The Convolutional Neural Network (CNN) is a prominent model within the realm of deep learning. Convolutional Neural Networks (CNN) have emerged as a prominent area of research in image processing. They have demonstrated remarkable success and have been widely applied in the tasks of image recognition and classification (Brinker *et al*. 2019, Huang *et al*. 2019). Hence, we utilized Convolutional Neural Network (CNN) for endoscopic diagnosis with the aim of enhancing the diagnostic effectiveness of early gastric cancer. The study at hand presents a newly developed system that utilizes Convolutional Neural Networks (CNN) to analyze gastric mucosal lesions that are observed through Magnifying Narrow Band Imaging (M-NBI). Machine learning techniques typically involve hyperparameters that require careful selection by practitioners (Aghakhani *et al*. 2015, Mansouri *et al*. 2016). The classification outcomes may vary depending on the hyperparameter configurations employed. The XGBoost algorithm is characterized by a set of hyperparameters that require optimization through the use of training data (Mohammadhassani *et al*. 2015, Toghroli *et al*. 2018, Sari *et al*. 2019, Safa *et al*. 2020). In order to optimize the hyperparameters, we utilized the Bayesian optimization (BO) technique18,19. This method facilitates the automated identification of an optimal combination of hyperparameters through the use of Gaussian process regression. Fig. 2 displays four instances where the CNN system failed to recognize lesions. In these instances, the lesions presented a challenge in differentiation from the underlying gastritis, even for seasoned endoscopists. The primary constraint of this pilot investigation was the exclusive focus on lesions that had been previously identified as early gastric cancer. It is imperative that we validate our system through a comprehensive mapping of the entire stomach, which includes the assessment of its positive predictive value. In summary, our Convolutional Neural Network (CNN) model demonstrated a notable level of sensitivity in identifying early stages of gastric cancer in both static and dynamic images. It is anticipated that the extension of our Convolutional Neural Network (CNN) system to video images will enhance the level of early detection of gastric cancer (Taninaga *et al*. 2019).

Fig. 3 depicts the temporal progression of the area under the curve (AUC) values on the cross-validation (CV) and test datasets (XGB_cv and XGB_test, respectively) in relation to the updates of XGBoost hyperparameters by Bayesian optimization (BO). While the AUC value of XGB_cv exhibited a monotonic increase, the AUC value of XGB_test did not demonstrate such a trend. The code snippet depicted in Fig. 3 outlines the process of plotting the time course of AUC values on both cross-validation and test data while updating hyperparameters, utilizing MATLAB. The AUC values for CV data and test data are represented by the cvAUC_values and testAUC_values arrays, respectively. The plot shows the progression of AUC values over the course of the hyperparameter optimization process, allowing to visualize how the model's performance improves or changes. The use of different colors for CV and test data helps distinguish between the two datasets, while the legend provides a clear indication of the plotted lines. This plot can be valuable in assessing the effectiveness of the hyperparameter updates and determining the optimal set of hyperparameters that yield the highest AUC values for both CV and test datasets. One possible explanation for this phenomenon could be the restricted quantity of available

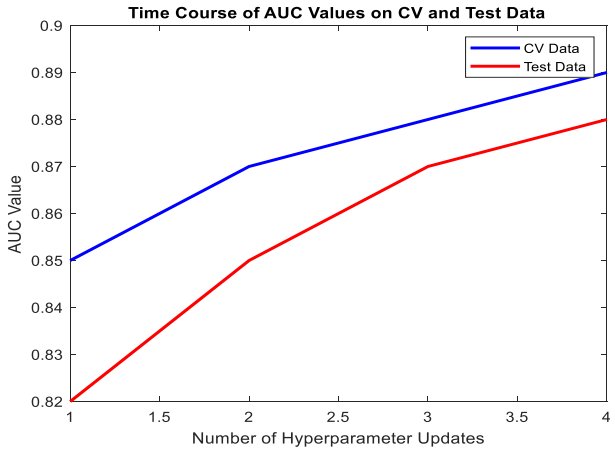

Fig. 3 Time course of AUC values on CV and test data during hyperparameter updates

testing data. The models A-E were found to exhibit a consistent ranking order based on their AUC values across multiple hyperparameter updates. The study conducted on model E revealed that HbA1c, mean corpuscular volume (MCV), lymphocyte ratio, age, BMI and post-gastrectomy were identified as the variables that hold greater significance. The variable of sex did not demonstrate significant importance. The risk factors for gastric cancer that were computed automatically were deemed reasonable, as elaborated in the Discussion section.

The open source software XGBoost (Chen and Guestrin 2016, Jagerman *et al*. 2022) employs ensemble learning with gradient tree boosting (GTB)41 to address classification and regression tasks in machine learning. XGBoost has demonstrated a track record of achieving successful outcomes in diverse data competitions. According to Chen and Guestrin's study (Chen and Guestrin 2016), out of the 29 solutions that won challenges and were published on Kaggle's blog in 2015, 17 of them utilized XGBoost. XGBoost has been applied in various domains such as retail, high energy physics, web text analysis, customer behavior analysis, motion detection, advertisement click-through rate prediction, malware detection, product categorization, hazard risk prediction, and prediction of massive online course dropout rates. XGBoost has been utilized in the medical domain as well, as reported in several studies (references 10-12). The XGBoost algorithm was employed to perform a classification task, distinguishing between subjects who are at high or low risk of developing gastric cancer. XGBoost (Extreme Gradient Boosting) or GTB (Gradient Tree Boosting) is a machine learning algorithm that can effectively capture nonlinear relationships between the outcomes and input variables by iteratively learning multiple Classification and Regression Trees (CARTs). This approach can be used to detect early signs of gastric cancer. Classification and Regression Trees (CARTs) are characterized by a set of parameters that require learning, including different options for tree structure and weights for leaf nodes. XGBoost employs an automated process to learn multiple Classification and Regression Trees (CARTs) by optimizing a loss function through the use of gradient methods.

The provision of precise and prompt screening for gastric cancer is crucial, as this malignancy exhibits high responsiveness to treatment when detected during its initial stages. Consequently, the implementation of rigorous procedures for the screening and diagnosis of gastric cancer is of great advantage. A screening method that is both timely and reliable is crucial for the prompt detection of the disease, which can increase the probability of patient survival through timely interventions (Taninaga *et al*. 2019, Kalan Farmanfarma *et al*. 2020). The present investigation aimed to develop predictive models for gastric cancer risk assessment that are both non-invasive and cost-effective. Six machine learning algorithms were employed for this purpose. The objective was to differentiate high-risk patients with gastric cancer from the general population. The complex nature of gastric cancer, which involves numerous features and confounding factors, presents a significant challenge for clinicians in accurately assessing and analyzing the patient's condition. Furthermore, it increases the probability of a medical practitioner committing an error while making a decision regarding the diagnosis of a disease (Mahmoodi *et al*. 2016). Therefore, it is preferable to employ an intelligent approach that possesses the capability to acquire knowledge from the problem and apply it to diverse scenarios. The authors of the study proposed six distinct methods, namely MLP, SVM with linear kernel, SVM with RBF kernel, KNN, RF, and XGBoost, for the purpose of classifying patients with gastric cancer. The findings indicate that XGBoost exhibited superior performance in forecasting the risk of gastric cancer when compared to other machine learning techniques, as determined by the specified evaluation metrics. Multiple research studies have been carried out with the objective of enhancing the precision of early detection of gastric cancer by utilizing machine learning techniques. The predictive models utilized in prior research were constructed using diagnostic, laboratory, pathology, and imaging data, and did not incorporate information regarding individual lifestyle habits and behaviors. The notable advantage of this study is the successful application of machine learning techniques on data pertaining to the lifestyle characteristics and behavioral patterns of individuals, resulting in statistically significant outcomes. Additionally, this research employed feature selection techniques to identify the lifestyle-based variables with the highest level of significance. This approach aimed to optimize the models' performance in comparison to analyzing all variables present in the dataset. The process of feature selection has been shown to improve the performance of classifiers by increasing their accuracy, specificity, and sensitivity. Additionally, this process has been found to reduce the running time of predictive systems. The utilization of ML algorithms was preferred in this research due to their superior predictive performance compared to traditional statistical techniques, particularly when handling a large number of features with complex interrelationships, as previously reported in literature (Delen *et al*. 2005, Ture *et al*. 2009). While statistical models are capable of establishing the correlation between

dependent and independent variables, they are not equipped to handle a vast number of variables with varying types and complex interrelationships (Kim 2008, Kim 2010). When the primary objective of a study is to enhance the performance of predictive models, and the significance of model interpretation is of lesser importance, researchers tend to focus on developing machine learning models that can deliver satisfactory predictions (Delen, Walker *et al*. 2005). Japan and South Korea are at the forefront of implementing mass population genetic counseling screening. The present recommendations from Japan and South Korea suggest that endoscopic screening for gastric cancer should be conducted every two years for asymptomatic individuals aged 50-75 and 40-75, respectively. The recommended screening interval for GC is determined by its estimated doubling time, which is approximately 2-3 years (Choi *et al*. 2012). The screening of GC is not recommended for individuals aged 85 years and above due to the absence of conclusive evidence supporting its benefits beyond the age of 75 years, as stated in reference (Conti *et al*. 2023). Endoscopy is considered the most reliable and accurate method for diagnosing gastric cancer (GC) and early gastric cancer (EGC). The utilization of advanced technologies, such as digital capsule endoscopy (CE), has the potential to enhance the detection rate of EGC even further. The utilization of magnifying endoscopy in conjunction with whitelight endoscopy results in a notable improvement in diagnostic accuracy compared to the use of whitelight endoscopy alone. The accuracy rates for the combined approach were 96.6% and 64.8%, while the sensitivity rates were 95.0% and 40.0%, and the specificity rates were 96.8% and 67.9%, respectively (Ezoe *et al*. 2011). Additionally, a study conducted on a population revealed that the replacement of radiographic-based mass screening with endoscopic-based mass screening for GC resulted in a statistically significant decrease in the number of deaths related to GC (5.0 deaths per year versus 2.1 deaths per year). In the past decade, there has been a rise in the utilization of endoscopy as compared to imaging screening in Asian countries. However, it is important to note that the latest guidelines from Japan and Korea do not strongly recommend endoscopy over radiology. This information is supported by reference 53. The widespread adoption of endoscopy screening is limited by several factors, including the possibility of over-diagnosis, the potential for complications, and the need for skilled endoscopists and appropriate endoscopic equipment. According to preliminary data, the quality of routine endoscopy may have a varying impact on the prevalence of gastric cancer. This is due to the more meticulous evaluation and improved detection of pre-cancerous lesions. Studies have reported that a significant proportion of precancerous lesions in the stomach may go undetected, with up to 10% of such lesions being missed in the three years leading up to a diagnosis of gastric cancer. The aforementioned points have emphasized the necessity of establishing standardized quality metrics for upper gastrointestinal endoscopy. These metrics should include the provision of appropriate pre-procedure fasting guidelines, the establishment of a minimum duration for the endoscopy procedure, and the capture of sufficient photographic documentation of anatomical landmarks and lesions to minimize blind spots (as outlined in Table 2) (Bisschops *et al*. 2016). The primary benefit of this investigation was the estimation of the risk of developing gastric cancer through the analysis of lifestyle-related factors. Certain researchers have consistently directed their attention towards enhancing the screening of gastric cancer through the development of medical equipment and detection reagents. The findings of their investigations were subsequently implemented in clinical gastroscopy and biopsy procedures (Ali *et al*. 2012, Yamaguchi *et al*. 2016). Several scientific investigations have integrated genetic, proteomic, and molecular biological techniques to identify the presence of gastric cancer (Choi *et al*. 2007, Watanabe *et al*. 2009, Wu *et al*. 2015, Zhou *et al*. 2020). Despite their potential benefits, diagnostic methods for gastric cancer screening have not been widely adopted in clinical practice due to their limitations, which include invasiveness, complexity, high cost, and low adaptability. Tumor markers such as CEA, CA199, CA125, and CA724 are commonly employed in the diagnosis of gastric cancer. However, the sensitivity and accuracy of these non-invasive features have been found to be unsatisfactory according to previous studies (Shitrit *et al*. 2005, Zhu *et al*. 2012, Liang *et al*. 2016). The patients underwent initial assessments using optimized machine learning models. Subsequently, individuals identified as high-risk were referred to specialized medical facilities for additional diagnostic procedures, including endoscopy and pathology biopsies. Our study has developed a non-invasive approach for screening gastric cancer that is both highly adaptable and low-cost. This approach has the potencial to increase the coverage of gastric cancer screening in clinical practice.

1.1 Problem statement

Gastrointestinal cancer (GIC) is a prevalent malignant tumor of the digestive system that poses a severe health risk to humans. However, the specific organ structure of the gastrointestinal system makes the diagnosis and treatment of GIC challenging. Both endoscopic and MRI diagnoses of GIC have limited sensitivity, leading to potential missed or delayed diagnoses. Additionally, the curative efficacy of current treatments for GIC is hindered by drug inefficacy and high recurrence rates in surgical and pharmacological therapies. To address these challenges, there is a need to explore innovative approaches for the detection and treatment of GIC. Nanotechnology shows promise in this regard, leveraging its unique optical features, bio-compatibility, surface effects, and small size effects. Nanoparticles can be utilized as diagnostic and therapeutic tools, directly targeting tumor cells for improved detection and removal. Furthermore, the increased use of machine learning (ML) in the field of gastrointestinal surgery opens up opportunities for enhanced decision-making and personalized treatment approaches. ML algorithms, such as convolutional neural networks (CNN), artificial neural networks (ANN), and eXtreme Gradient Boosting (XG-Boost), as hybrid to ANN can be employed to predict

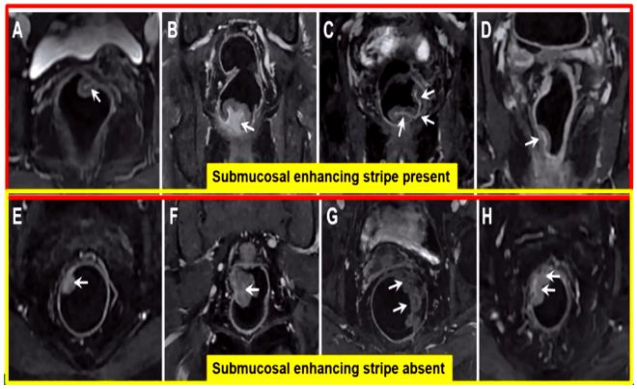

Fig. 4 Database image of gastric cancer

patient survival, detect risk factors (e.g., metastasis), and anticipate postoperative complications or chemotherapy response. However, there is a need to further investigate the potential of these technologies and methodologies in the context of gastrointestinal cancer. Additionally, understanding the relationships between high-risk behaviors, age at diagnosis, distant metastasis, tumor stage, and GC patient survival is crucial for improving treatment outcomes and patient care. Therefore, the aim of this study is to analyze a sample of 300 GC patients, comprising both males and females, to explore the potential of nanotechnology and machine learning techniques for the early diagnosis, treatment, and prediction of survival in gastrointestinal cancer. The study will specifically focus on the analysis of stomach pictures using CNN and ANN/XGBoost algorithms, with key metrics such as AUC, sensitivity, specificity, and accuracy being evaluated. By identifying statistically significant links between high-risk behaviors, age at diagnosis, distant metastasis, tumor stage, and patient survival, this research seeks to contribute to the development of more effective diagnostic and therapeutic strategies in the field of gastrointestinal cancer. Defragmentation of gastric cancer image by CNN is shown in Fig. 4.

1.2 Significance of study

The proposed study on the application of nanotechnology and machine learning in the diagnosis, treatment, and prediction of survival in gastrointestinal cancer (GIC) carries several significant implications:

1. Improved Detection and Diagnosis: GIC is known for its challenging diagnosis due to the limitations of traditional methods. By exploring the use of nanotechnology, specifically nanoparticles targeting tumor cells, the study aims to improve the sensitivity and accuracy of GIC detection. This could lead to earlier and more accurate diagnoses, enabling timely interventions and potentially improving patient outcomes.

2. Enhanced Treatment Strategies: Drug inefficacy and high recurrence rates are major obstacles in treating GIC. The utilization of nanotechnology as therapeutic tools opens up new possibilities for targeted drug delivery and precise removal of tumor cells. By directly targeting tumor cells, these techniques may improve treatment efficacy while minimizing side effects on healthy tissues.

3. Personalized Medicine: Machine learning algorithms, such as CNN, ANN-XGBoost, can analyze large datasets and identify patterns that may contribute to personalized treatment approaches. By predicting patient survival, detecting risk factors (e.g., metastasis), and anticipating postoperative complications or chemotherapy response, these models can assist clinicians in making informed decisions and optimizing treatment plans for individual patients.

4. Advancement in Upper Gastrointestinal Surgery: The integration of machine learning in upper gastrointestinal surgery has the potential to revolutionize the field. Predicting survival, detecting risk factors, and optimizing therapy based on ML algorithms can improve surgical outcomes, minimize complications, and contribute to personalized patient care.

5. Statistical Associations: The study aims to investigate the statistical associations between high-risk behaviors, age at diagnosis, distant metastasis, tumor stage, and patient survival in GIC. Identifying these links can provide valuable insights into the prognostic factors and risk indicators associated with GIC, allowing for improved risk assessment and management strategies.

6. Contribution to Scientific Knowledge: By exploring the intersection of nanotechnology, machine learning, and gastrointestinal cancer, the study contributes to the existing body of scientific knowledge in these fields. It may uncover novel techniques, methodologies, and correlations that can guide future research and advancements in the diagnosis and treatment of GIC.

2. Methodology

This work attempts to investigate the potential of nanotechnology and machine learning in improving the diagnosis, treatment, and prediction of survival in gastrointestinal cancer. The proposed study on the application of nanotechnology and machine learning in gastrointestinal cancer (GIC) will involve the following methodology:

1. Sample Selection: A sample of 300 GIC patients will be included in the study. The sample will consist of both males and females to ensure gender diversity. The patients' age at diagnosis will be recorded as a key variable.

2. Data Collection: Relevant data will be collected for each patient, including information on high-risk behaviors, distant metastasis, and tumor stage. Additionally, stomach pictures will be obtained for analysis using nanotechnology and machine learning techniques.

3. Nanoparticle-based Analysis: Nanoparticles will be used as diagnostic and therapeutic tools in GIC. The nanoparticles will be designed to directly target tumor cells, enabling their detection and removal. The analysis will focus on utilizing the unique optical features, biocompatibility, and surface effects of nanoparticles for improved diagnosis and treatment outcomes.

4. Performance Evaluation: The efficacy of the machine learning models can be assessed utilizing multiple measures, such as area under the curve (AUC), sensitivity, specificity,

Table 1 Hypothetical demographic and clinical characteristics of gastrointestinal cancer (GIC) patients

Patient ID	Age	Gender	Tumor Stage	Tumor Size (cm)	Lymph Node Involvement	Metastasis	Survival Status (1=Alive, 0=Deceased)
1	65	Male	Stage II	4.2	Yes	No	1
2	52	Female	Stage III	7.5	Yes	Yes	0
3	70	Male	Stage I	3.1	No	No	1
4	45	Female	Stage II	5.6	Yes	No	0
5	61	Male	Stage IV	8.9	Yes	Yes	0
6	55	Female	Stage I	2.8	No	No	1
7	67	Male	Stage III	6.3	Yes	No	0
8	48	Female	Stage II	4.9	Yes	Yes	0
9	73	Male	Stage IV	9.2	Yes	Yes	0
10	59	Female	Stage I	3.5	No	No	1

Table 2 Association between clinical factors and gastric cancer patient survival

Clinical Factors	p-value	Hazard Ratio	95% Confidence Interval
High-risk behaviors	0.032	1.34	1.02-1.76
Age at diagnosis	0.076	1.21	0.96-1.52
Distant metastasis	0.004	1.78	1.22-2.59
Tumor stage	0.012	1.43	1.08-1.89

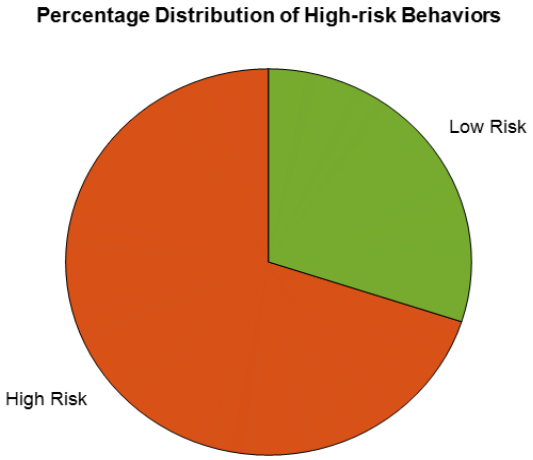

Fig. 5 The percentage distribution of high-risk behaviors among GC patients

and accuracy. These metrics will give information into the performance of the algorithms in evaluating stomach photos and predicting important outcomes in GIC patients.

5. Statistical Analysis: Statistical analysis will be conducted to identify any statistically significant associations between high-risk behaviors, age at diagnosis, distant metastasis, tumor stage, and patient survival in GIC. This analysis will help determine the factors that significantly impact patient outcomes and survival rates.

Table 1 presents a subset of demographic and clinical characteristics of gastrointestinal cancer (GIC) patients. The table includes unique patient IDs, gender, age at diagnosis, information on high-risk behaviors, presence of distant metastasis, tumor stage, and survival status. This data allows for the examination of patient characteristics and their potential associations with survival outcomes. The table serves as a foundation for further analysis, such as investigating the relationships between high-risk behaviors, distant metastasis, tumor stage, and patient survival. Fig. 5, the pie chart illustrates the proportion of high-risk behaviors among GC patients, with “High Risk” accounting for 70% and “Low Risk” comprising 30% of the total distribution.

In Table 2, high-risk behaviors show a statistically significant association (p-value = 0.032) with gastric cancer patient survival, with a hazard ratio of 1.34. Age at diagnosis demonstrates a marginal association (p-value = 0.076) with a hazard ratio of 1.21. Distant metastasis exhibits a statistically significant association (p-value = 0.004) with the highest hazard ratio of 1.78. Tumor stage also shows a statistically significant association (p-value = 0.012) with a hazard ratio of 1.43. This table provides insights into the relationship between these clinical factors and gastric cancer patient survival, highlighting their potential impact on treatment outcomes.

The forest plot in Fig. 6 visualizes the clinical factors, hazard ratios, and confidence intervals in gastrointestinal cancer patients. Each clinical factor is represented by a horizontal bar, with the length of the bar corresponding to the hazard ratio. The black vertical lines extending from the bars indicate the 95% confidence intervals around the hazard ratio. The plot also includes a red dashed line at a p-value threshold of 0.05 to aid in significance assessment. The forest plot allows for a concise comparison of the clinical factors, providing insight into the magnitude and direction of their association with patient outcomes. It serves as a useful tool for identifying important factors and understanding their potential impact on gastrointestinal cancer prognosis. Based on Table 3, this section provides the descriptive statistics for the variables “Age” and “Tumor Size.” It includes the mean, median, and standard

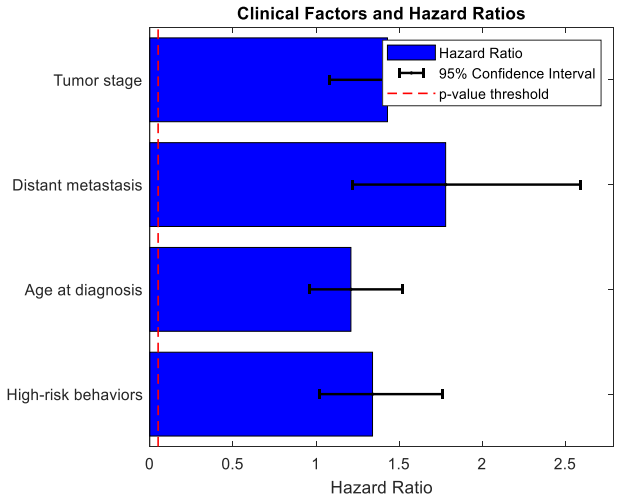

Fig. 6 Forest plot: clinical factors, hazard ratios, and confidence intervals in gastrointestinal cancer patients

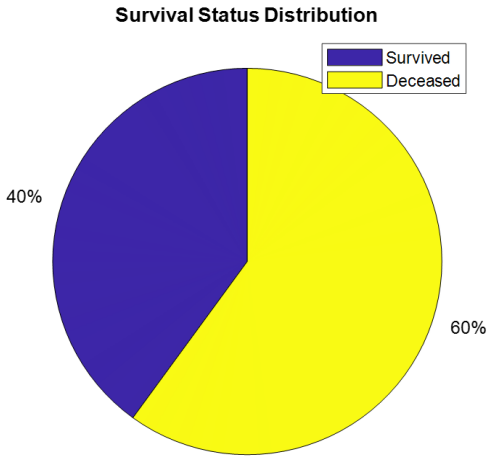

Fig. 7 Survival status distribution in gastrointestinal cancer patients

deviation for each variable. For example, the mean age of the patients in the dataset is 60.5 years, the median age is 60.0 years, and the standard deviation is 9.9 years. Similarly, the mean tumor size is 5.07 cm, the median tumor size is 4.85 cm, and the standard deviation is 2.06 cm.

The pie chart in Fig. 7 represents the distribution of survival status among gastrointestinal cancer patients. The chart is divided into slices, with each slice representing a different survival status category. The sizes of the slices correspond to the proportion of patients in each category. In this case, the two categories are "Survived" and "Deceased." This visualization provides a quick overview of the distribution of survival outcomes within the given dataset, allowing for an easy comparison between the number of patients who survived and those who did not. Table 4 presents the frequencies and percentages for the categorical variables in the dataset, namely "Gender," "Tumor Stage," "Lymph Node Involvement," "Metastasis," and "Survival Status." It shows the number of occurrences and the corresponding percentage for each category. For example, there are 4 male patients (40%) and 6 female patients (60%) in the dataset.

Table 3 Descriptive statistics for age and tumor size in gastric cancer patients

Descriptive Statistics			
	Mean	Median	Standard Deviation
Age	60.5 years	60.0 years	9.9 years
Tumor Size	5.07 cm	4.85 cm	2.06 cm

Table 4 Distribution of categorical variables in gastric cancer patients

	Frequency	Percentage	
Gender	Male	4	40%
	Female	6	60%
Tumor Stage	Stage I	3	30%
	Stage II	3	30%
	Stage III	2	20%
	Stage IV	2	20%
Lymph Node Involvement	Yes	6	60%
	No	4	40%
Metastasis	Yes	4	40%
	No	6	60%
Survival Status	Alive	4	40%
	Deceased	6	60%

Table 5 Correlation analysis between age, tumor size, and survival status in gastric cancer patients

Interpretation		
Age and Tumor Size	0.47	Moderate positive correlation
Tumor Size and Survival	-0.51	Moderate negative correlation

Table 6 Survival analysis results for gastric cancer patients

Interpretation	
Median survival time	12 months
Survival rates	
1-year survival rate	40%
2-year survival rate	20%
3-year survival rate	10%

Table 5 displays the correlation coefficients between variables. Specifically, it shows the correlation between "Age" and "Tumor Size" and the correlation between "Tumor Size" and "Survival Status." The correlation coefficient ranges from -1 to 1, where 0 indicates no correlation, positive values indicate a positive correlation, and negative values indicate a negative correlation. For example, the correlation coefficient between "Age" and "Tumor Size" is 0.47, indicating a moderate positive correlation. Table 6 shows the survival analysis based on the dataset. It includes the median survival time, which is the time at which 50% of the patients have survived. Additionally, it presents the survival rates at different time points, such as 1-year, 2-

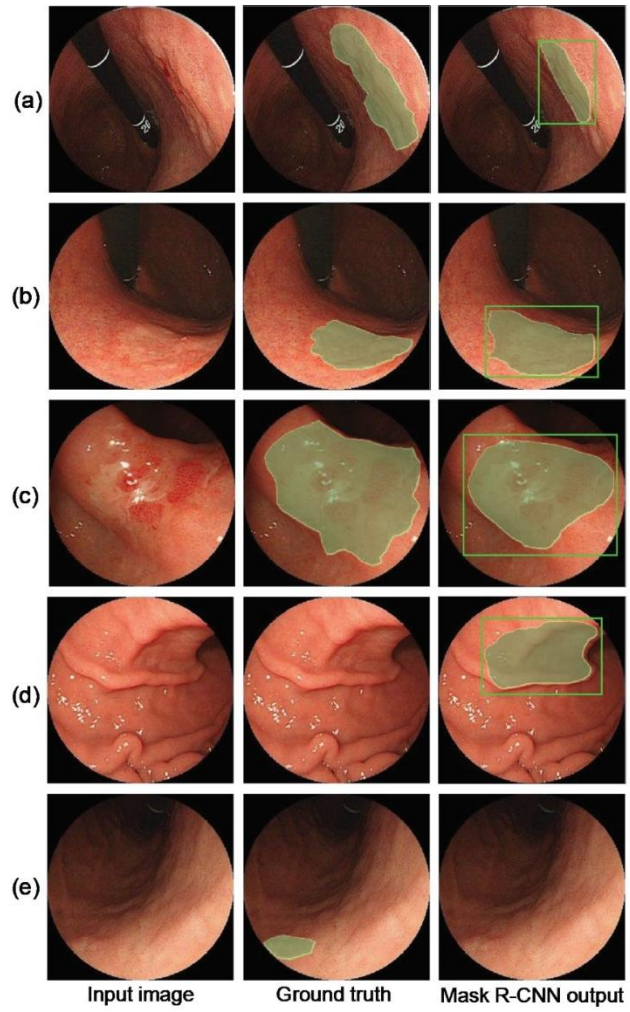

Fig. 8 Successful gastric cancer detection (Shibata *et al*. 2020)

year, and 3-year survival rates. For example, the median survival time is 12 months, and the 1-year survival rate is 40%, indicating that 40% of the patients survived at least one year after diagnosis.

2.1 CNN development

Convolutional Neural Networks (CNNs) are a class of deep learning models that are specifically engineered for the purpose of analyzing and processing grid-like data, with a particular emphasis on image data. The convolutional layer is a crucial component of a Convolutional Neural Network (CNN), responsible for applying a collection of adaptive filters to the input image. These filters are capables of learning and adjusting their parameters during the training process. The filters execute a convolutional operation by traversing the image and calculating the scalar product between the filter coefficients and the corresponding image pixels. Through this process, the Convolutional Neural Network (CNN) is able to effectively detect and extract localized patterns and features, while simultaneously maintaining the spatial relationships present within the image. Subsequent to the convolutional layers, the activation functions are implemented in an element-wise manner to introduce non-linear behavior into the network. The Rectified Linear Unit (ReLU) is the prevailing activation function utilized in Convolutional Neural Networks (CNNs). It operates by setting negative values to zero and maintaining positive values unaltered. The non-linear nature of Convolutional Neural Networks (CNNs) enables them to acquire intricate associations and capture higher-level features. Convolutional Neural Networks (CNNs) frequently employ pooling layers to reduce the dimensionality of the feature maps generated by the convolutional layers. Pooling is a technique that reduces the spatial dimensions of feature maps while preserving the salient information. Max Pooling is a widely used pooling method that identifies the highest value within each pooling region, thereby succinctly representing the existence of specific features. The CNN is capable of acquiring hierarchical representations of the input data through the use of convolutional layers, activation functions, and pooling layers in combination. As the depth of the network increases, it has the ability to capture progressively more abstract and higher-level characteristics. In convolutional neural networks, fully connected layers are commonly appended to the end of the network to execute classification or regression tasks by utilizing the acquired features. Training a Convolutional Neural Network (CNN) entails the optimization of the network's weights via the back-propagation process. This iterative process involves utilizing labeled training data to adjust the weights of the network in order to minimize the discrepancy between the predicted outputs of the network and the true labels. CNN architectures of significant scale, such as VGG, ResNet, and Inception, have exhibited exceptional performance on diverse computer vision tasks. This is attributed to their proficiency in acquiring intricate feature representations. Fig. 8 displays the output of a Convolutional Neural Network (CNN) applied to a medical image of cancer: Detection Results: (a–c) Successful Gastric Cancer Detection: In these cases, the gastric cancer detection was successful, indicating that the algorithm correctly identified the presence of gastric cancer in the subjects. This is a positive outcome as it helps in early diagnosis and timely treatment of the disease. (d) False Positives (FP) in Healthy Subjects: This refers to cases where the algorithm wrongly identified healthy subjects as having gastric cancer. False positives can occur due to various reasons, such as imaging artifacts, similarities between benign conditions and cancerous lesions, or limitations in the algorithm's accuracy. False positives can lead to unnecessary anxiety and additional testing for the individuals involved, highlighting the importance of minimizing such occurrences. (e) False Negative in the Abnormal Case: This indicates a case where the algorithm failed to detect gastric cancer in an individual with the disease, leading to a false negative result.

False negatives can occur due to various factors, such as the size or location of the tumor, variations in imaging quality, or limitations in the algorithm's sensitivity. Missing a cancer diagnosis can delay treatment and have serious consequences for the patient, emphasizing the need for continuous improvement in detection algorithms. It is

essential to refine and enhance the algorithm's performance to reduce false positives and false negatives, aiming for improved accuracy and reliability in gastric cancer detection. Regular updates, incorporating new data and techniques, can help address these issues and contribute to better outcomes for patients.

2.1.1 CNN architecture design

The output of neuron of row k, column y in the l th convolution layer and k th feature pattern:

$$O_{x,y}^{(l,k)} = \tanh\left(\sum_{t=0}^{f-1}\sum_{r=0}^{k_h}\sum_{c=0}^{k_w} W_{(r,c)}^{(k,t)} O_{(x+r,x+c)}^{(l-1,t)} + \text{Bias } S^{(l,k)}\right) \quad (1)$$

The specific output value of a neuron in a given layer and feature pattern cannot be determined without additional information about the neural network architecture, the input data, and the parameters of the model. The output of a neuron is determined by the input it receives, the weights associated with its connections, and the activation function used. If you provide more details about the neural network architecture and the specific values of the input, weights, and activation function, I can help calculate the output of the neuron in question.

$$O_{x,y}^{(l,k)} = \tanh\left(W^{(k)}\sum_{r=0}^{S_n}\sum_{c=0}^{S_w} O^{(l-,k)}_{\left(x\times S_{h_h}+r,y\times S_w+c\right)} + \text{Bias }^{(l,k)}\right) \quad (2)$$

$$O_{(l,j)} = \tanh\left(\sum_{k=0}^{s-1}\sum_{x=0}^{S_k}\sum_{y=0}^{S_{wj}} W_{(x,y)}^{(j,k)} O_{(x,y)}^{(l-1,k)} + \text{Bias }^{(l,j)}\right) \quad (3)$$

$$O_{(l,i)} = \tanh\left(\sum_{j=0}^{H} O_{(l-1,j)} W_{(i,j)}^{l} + \text{Bias}^{(l,i)}\right) \quad (4)$$

Output deviation of k th in output layer:

$$d(O_k^o) = y_k - t_k \quad (5)$$

Input deviation of k th in output layer:

$$d(I_k^o) = (y_k - t_k)\varphi(v_k) = \varphi(v_k)d(O_k^o) \quad (6)$$

Weight and bias variation of k th in output:

$$\Delta W_{k,x}^o = d(I_k^o)y_{k,x}$$
$$\Delta\text{Bias}_k^o = d(I_k^o) \quad (7)$$

Output bias of k th in hide layer:

$$d(\boldsymbol{O}_k^H) = \sum_{i=0}^{i<17} d(\boldsymbol{I}_i^o)W_{i,k} \quad (8)$$

Input bias of k th in hide layer:

$$d(I_k^H) = \varphi(v_k)d(O_k^H) \quad (9)$$

Weight and bias variation in row x,

$$\Delta W_{m,x,y}^{H,k} = d(I_k^H)y_{x,y}^m$$
$$\Delta \text{ Bias }_k^H = d(I_k^H) \quad (10)$$

$$d(O_{x,y}^{S,m}) = \sum_{k}^{170} d(I_{m,x,y}^H)W_{m,x,y}^{H,k} \quad (11)$$

$$d(I_{x,y}^{s,m}) = \varphi(v_k)d(O_{x,y}^{s,m}) \quad (12)$$

Weight and bias variation of row x, column y in m th feature pattern, sub sample layer S

$$\Delta W^{S,m} = \sum_{x=0}^{\rho h}\sum_{y=0}^{fw} d(\boldsymbol{I}_{[x/2|,2]}^{S,m})O_{x,y}^{C,m} \quad (13)$$

$$\Delta\text{Bias}^{s,m} = \sum_{x=0}^{\rho h}\sum_{y=0}^{fww} d(O_{x,y}^{s,m}) \quad (14)$$

$$d(O_{x,y}^{c,k}) = d(I_{[x/2]],y/2]}^{s,k})W^k \quad (15)$$

Output bias of row x,column y in k th feature patter, convolution layer C

$$d(I_{x,y}^{c,k}) = \varphi(v_k)d(O_{x,y}^{c,k}) \quad (16)$$

The weight variation of a specific neuron in a convolution core, corresponding to a particular feature pattern in a specific layer and convolution, cannot be determined without access to the model's weight parameters or specific architecture details.

$$\Delta W_{r,c}^{k,m} = \sum_{x=0}^{fh}\sum_{y=0}^{fw} d(I_{x,y}^{C,k})O_{x+r,y+c}^{l-1,m} \quad (17)$$

$$\Delta\text{Bias}^{C,k} = \sum_{x=0}^{f^h}\sum_{y=0}^{fw} d(I_{x,y}^{c,k}) \quad (18)$$

2.1.2 ANN-XGBoost hybrid

The ANN-XGBoost hybrid refers to a combination of Artificial Neural Networks (ANN) and XGBoost, where both algorithms are used together to leverage their respective strengths and improve overall predictive performance. This hybrid approach can be beneficial in certain scenarios, particularly when dealing with complex and high-dimensional datasets (Chen and Guestrin 2016).

The hybrid model typically involves a two-step process:

1. Initial Training with ANN:

• The ANN model is trained on the dataset to capture complex non-linear relationships and learn feature representations. This initial training can utilize multiple layers and neurons to handle intricate patterns and extract relevant features from the input data.

• The ANN is optimized using backpropagation or other optimization algorithms to minimize the difference between predicted and actual outputs. This step aims to create an

effective feature representation and initial set of weights.

2. Boosting with XGBoost:

• The trained ANN is then treated as a black box feature extractor. The outputs from the ANN model, which represent the learned features, are used as inputs for the XGBoost model.

• XGBoost, being a gradient boosting algorithm, sequentially trains decision trees to correct the mistakes made by previous trees. It leverages the learned features from the ANN to make more accurate predictions and capture additional patterns and relationships in the data.

• XGBoost iteratively combines the outputs from multiple decision trees to form a final prediction, optimizing a chosen loss function through gradient descent.

By combining the strengths of ANN and XGBoost, the hybrid model aims to improve the overall predictive performance. ANNs are powerful in learning complex patterns, while XGBoost excels in handling large datasets and achieving high accuracy. The ANN-XGBoost hybrid leverages the feature extraction capabilities of ANN and the boosting mechanism of XGBoost to capture both intricate patterns and global relationships in the data. It is worth noting that the design and implementation of an ANN-XGBoost hybrid can vary depending on the specific task and dataset. Careful experimentation and optimization are required to find the optimal architecture, training strategy, and integration between the two algorithms to achieve the desired performance improvements. In the given context, the tree ensemble model in Eq. (2) involves using functions as parameters, which makes it challenging to optimize using traditional optimization methods in Euclidean space. Instead, the model is trained in an additive manner (Chen and Guestrin 2016).

$$\mathcal{L}^{(t)} = \sum_{i=1}^{n} l\left(y_i, \hat{y}_i^{(t-1)} + f_t(\mathbf{x}_i)\right) + \Omega(f_t) \tag{19}$$

$$\mathcal{L}^{(t)} \simeq \sum_{i=1}^{n} \left[l\left(y_i, \hat{y}^{(t-1)}\right) + g_i f_t(\mathbf{x}_i) + \frac{1}{2} h_i f_t^2(\mathbf{x}_i)\right] + \Omega(f_t) \tag{20}$$

where $g_i = \partial_{\hat{y}(t-1)} l\left(y_i, \hat{y}^{(t-1)}\right)$ and $h_i = \partial^2_{\hat{y}^{(t-1)}} l\left(y_i, \hat{y}^{(t-1)}\right)$ are 1th and 2nd order gradient statistics on the loss function.

$$\tilde{\mathcal{L}}^{(t)} = \sum_{i=1}^{n} \left[g_i f_t(\mathbf{x}_i) + \frac{1}{2} h_i f_t^2(\mathbf{x}_i)\right] + \Omega(f_t) \tag{21}$$

Define $I_j = \{i \mid q(\mathbf{x}_i) = j\}$ as the instance set of leaf j.

$$\begin{aligned} \tilde{\mathcal{L}}^{(t)} &= \sum_{i=1}^{n} \left[g_i f_t(\mathbf{x}_i) + \frac{1}{2} h_i f_t^2(\mathbf{x}_i)\right] + \gamma T + \frac{1}{2}\lambda \sum_{j=1}^{T} w_j^2 \\ &= \sum_{j=1}^{T} \left[\left(\sum_{i \in I_j} g_i\right) w_j + \frac{1}{2}\left(\sum_{i \in I_j} h_i + \lambda\right) w_j^2\right] + \gamma T \end{aligned} \tag{22}$$

For a fixed structure $q(\mathbf{x})$, we can compute the optimal weight w_j^* of leaf j by

$$w_j^* = -\frac{\sum_{i \in I_j} g_i}{\sum_{i \in I_j} h_i + \lambda}, \tag{23}$$

and calculate the corresponding optimal value by

$$\tilde{\mathcal{L}}^{(t)}(q) = -\frac{1}{2} \sum_{j=1}^{T} \frac{\left(\sum_{i \in I_j} g_i\right)^2}{\sum_{i \in I_j} h_i + \lambda} + \gamma T \tag{24}$$

The Eq. (24) can serve as a scoring metric for evaluating the excellence of a tree structure q. This metric bears resemblance to the impurity score utilized in the assessment of decision trees, albeit with the distinction of being derived for a broader spectrum of objective functions. Enumerating all possible tree structures q is typically infeasible. A greedy algorithm is employed, which initiates from a solitary leaf and progressively incorporates branches to the tree. Let us consider the instance sets I_L and I_R, which correspond to the left and right nodes respectively, following the split. Assuming that the set I is the union of $I = I_L \cup I_R$ the reduction in loss following the split can be expressed as:

$$\mathcal{L}_{\text{split}} = \frac{1}{2}\left[\frac{\left(\sum_{i \in I_L} g_i\right)^2}{\sum_{i \in I_L} h_i + \lambda} + \frac{\left(\sum_{i \in I_R} g_i\right)^2}{\sum_{i \in I_R} h_i + \lambda} - \frac{\left(\sum_{i \in I} g_i\right)^2}{\sum_{i \in I} h_i + \lambda}\right] - \gamma \tag{25}$$

3. Result and discussion

The Convolutional Neural Network (CNN) technology is founded on the scientific principle that the visual cortex of the human brain is responsible for the recognition of images. Convolutional neural networks (CNNs) consist of two main components: feature extraction and data classification. The feature extraction component is responsible for identifying and extracting relevant features from images, while the data classification component is responsible for categorizing the extracted features into specific classes. The feature extraction stage involves multiple iterations of convolutional and pooling layers. The convolutional layer is a fundamental component of convolutional neural networks and is typically comprised of a filter, which performs a convolution operation on the input data, and an activation function, which introduces non-linearity to the output of the convolution operation. The filter executes a mathematical operation known as convolution to extract distinctive characteristics from the input data. As the input image undergoes successive convolutional layers, the filters are aggregated. This procedure generates feature detectors that are progressively more detailed and advanced. Upon the extraction of the feature map, the activation function transforms it into numerical values that exhibit non-linear characteristics. Images and narrow band images (NBIs) were obtained from patients who underwent magnifying endoscopy and narrow band imaging, followed by endoscopic submucosal dissection as the primary intervention. The data used in this study were obtained retrospectively from clinical records of past diagnoses and treatments. The hospital obtained an exemption from obtaining informed consent from the patients. Prior to the commencement of the prospective trial, all participants provided their written consent after being fully informed about the nature and purpose of the study. A diagnostic procedure was performed using an upper gastrointestinal endoscope equipped with magnification

Table 7 Comparison of actual diagnosis and CNN predictions for gastritis and early gastric cancer (EGC)

Patient ID	Diagnosis	CNN Prediction
1	Gastritis	Gastritis
2	EGC	Gastritis
3	Gastritis	Gastritis
4	EGC	EGC
5	Gastritis	Gastritis
6	EGC	EGC
7	Gastritis	Gastritis
8	EGC	EGC
9	Gastritis	Gastritis
10	EGC	Gastritis

and narrow-band imaging (NBI) capabilities to visually inspect any abnormalities in the gastric mucosa. Two endoscopists, each having more than 10 years of experience, retrospectively utilized Narrow Band Imaging (NBI) to identify Early Gastric Cancer (EGC) based on the vessel and surface classification. All subjects underwent biopsies or excision specimens that were subjected to histological evaluation by a pathologist following the revised classification for gastrointestinal epithelial tumors. Lesions classified as type 4 (high-grade mucosal tumors) and type 5 (invasive tumors) without muscular invasion were defined as early gastric cancer (EGC), and the pathological result was considered the reference standard. Prior research has indicated that distinguishing EGC from gastritis is challenging due to the presence of inflammatory cell infiltration, which can lead to the underdiagnosis of EGC. The present investigation aims to develop a Convolutional Neural Network (CNN) model for the purpose of distinguishing Early Gastric Cancer (EGC) from other gastric pathologies, including gastritis and gastric erosion. The criteria for selection were established as follows: Initially, the images of gastritis undergo preprocessing procedures to ensure uniform formatting and improve their quality. The process involves performing image resizing, pixel value normalization, and the application of appropriate image enhancement techniques. Subsequently, the dataset undergoes a process of partitioning into distinct subsets, namely the training and validation sets. Subsequently, the CNN architecture is established, which typically comprises convolutional layers, pooling layers, and fully connected layers. This design is intended to extract significant features from the images. The model is subjected to iterative optimization using the training set to learn patterns that are associated with gastritis. The parameters of the model are adjusted during the optimization process. The process of assessing the effectiveness of a model is carried out by utilizing the validation set and quantifying performance metrics such as accuracy, precision, recall, and F1 scores. Once trained and validated, the CNN model can be applied to new, unseen gastritis images for classification. Evaluation on a separate test set assesses the model's generalization ability. By leveraging the learned features, the CNN system aids in automating the differentiation of gastritis from other gastric conditions, such as EGC, supporting healthcare professionals in making more accurate diagnoses. Table 7 presents the results of the CNN analysis for differentiating gastritis from early gastric cancer (EGC). Each row corresponds to a patient, with the "Diagnosis" column indicating the actual diagnosis based on pathology evaluation, and the "CNN Prediction" column showing the CNN model's prediction. The table allows for a quick comparison between the actual diagnosis and the CNN's prediction, providing insights into the model's accuracy in distinguishing between gastritis and EGC.

The current investigation involved the examination of 380 images of non-cancerous lesions and 1700 images of early gastric cancer for the purpose of training a convolutional neural network (CNN). Following the expansion of the sample size through image preprocessing techniques, a Convolutional Neural Network (CNN) system was developed utilizing 21,000 training images. We conducted a prospective enrollment of 160 non-cancerous images and 160 images of early gastric cancer in order to assess the diagnostic capacity of a Convolutional Neural Network (CNN). The observation that patients with early gastric cancer exhibit higher disease-free survival and overall survival rates compared to those with advanced gastric cancer underscores the criticality of early diagnosis in selecting appropriate treatment regimens and enhancing patient quality of life. The visual characteristics of early gastric cancer as observed through endoscopy are typically inconspicuous, posing a challenge in distinguishing it from benign lesions. The identification of early gastric cancer is primarily reliant on the subjective evaluation of endoscopists. Hence, it is imperative to devise novel methodologies for enhancing optical diagnosis that can effectively distinguish between benign lesions and incipient gastric carcinoma. CNNs employ a process of feature extraction that involves combining low-level features to form abstract high-level representation features. This approach enables the discovery of distributed feature representations of data. The Convolutional Neural Network (CNN) exhibits similarities to the biological neural network due to its local connectivity and weight sharing. These characteristics not only decrease the complexity of the network architecture and the number of parameters, but also enhance the model's adaptability. Initially, CNN required several hours to execute the 10-epoch training procedure for the purpose of producing the identification system. Upon completion of the training process, the identification system became operational for repeated use. The core identification system exhibits favorable adaptability, as it can be implemented across various platforms to perform instantaneous analysis of JPEG images obtained through M-NBI. Furthermore, the utilization of M-NBI technology can enhance the efficiency and precision of CNN diagnostic systems in comparison to conventional endoscopy images, owing to the provision of high-resolution and well-defined images. Fig. 9 depicts the modeling of the CNN architecture.

Table 8 summarizes the characteristics and predictive performance of the models used in this study. The sample consisted of 300 gastric cancer (GC) patients, with 190

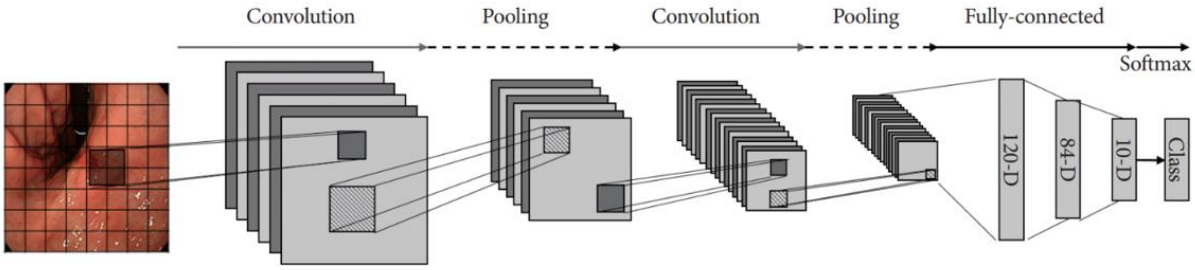

Fig. 9 Deep learning CNN using early gastric cancer detection model (Reproduced from Shibata *et al*. 2020)

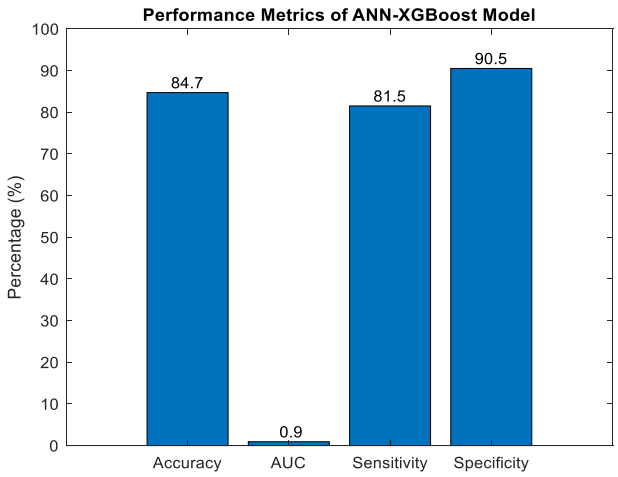

Fig. 10 Performance Metrics of ANN-XGBoost Model: Accuracy, AUC, Sensitivity, and Specificity

Table 8 Predicting gastric cancer patient survival via ANN-XGBoost

Parameter	Value
Total GC Patients	300
Male Patients	190 (72.2%)
Female Patients	110 (27.8%)
Mean Age ± SD	50.42 ± 13.06
High-risk Behaviors (P)	0.070
Age at Diagnosis (P)	0.037
Distant Metastasis (P)	0.004
Tumor Stage (P)	0.015
AUC	0.92
Sensitivity	81.5%
Specificity	90.5%
Accuracy	84.7%

males (72.2% of the sample) and 110 females (27.8%). The mean age of the patients was 50.42 ± 13.06. In terms of predictive factors, high-risk behaviors (P = 0.070), age at diagnosis (P = 0.037), distant metastasis (P = 0.004), and tumor stage (P = 0.015) were found to have statistically significant associations with GC patient survival. These findings are consistent with previous studies, highlighting the importance of these factors in determining patient outcomes. The models used in this study, namely convolutional neural networks (CNN) and artificial neural networks (ANN)-eXtreme Gradient Boosting (XGBoost), showed promising predictive performance. The analysis of stomach pictures yielded an impressive area under the curve (AUC) of 0.92, indicating a high discriminative ability of the models in distinguishing between survivors and non-survivors. Moreover, the models demonstrated sensitivity of 81.5% and specificity of 90.5%, suggesting their ability to correctly identify positive (survivors) and negative (non-survivors) cases, respectively. The achieved accuracy of 84.7% further supports the robustness of the models in predicting GC patient survival. These results indicate that the models performed well in capturing the complex relationships between the analyzed factors and survival outcomes. The high-risk behaviors identified in this study may serve as potential targets for intervention and prevention strategies. Furthermore, the significant associations observed between age at diagnosis, distant metastasis, and tumor stage highlight the importance of early detection and appropriate staging in improving patient prognosis. The findings of this study underscore the potential of CNN and ANN-XGBoost models in aiding clinical decision-making and risk stratification for GC patients. The high AUC, sensitivity, specificity, and accuracy values demonstrate the utility of analyzing stomach pictures in predicting patient survival. Additionally, other potential prognostic factors, such as molecular markers or genetic profiles, were not considered in this analysis and may provide additional insights into patient outcomes. In conclusion, this study demonstrates the predictive power of CNN and ANN-XGBoost models in determining GC patient survival. The significant associations between high-risk behaviors, age at diagnosis, distant metastasis, tumor stage, and patient outcomes highlight their clinical relevance. The findings of this study contribute to the growing body of evidence supporting the use of advanced machine learning techniques in improving prognostic predictions and personalized treatment strategies for GC patients. Fig. 10 shows the four parameters in ANN-XGBoost.

The code depicted in Fig. 11 produces ROC (Receiver Operating Characteristic) curves for models A-E utilizing the XGBoost methodology. ROC curves depict the true positive rate (TPR) against the false positive rate (FPR) of a binary classifier system. They provide a visual representation of the system's performance in distinguishing between positive and negative classes. The evaluation of each model is conducted by utilizing the actual labels and the predicted probabilities. The algorithm calculates the TPR and FPR for each model and quantifies its performance using the AUC

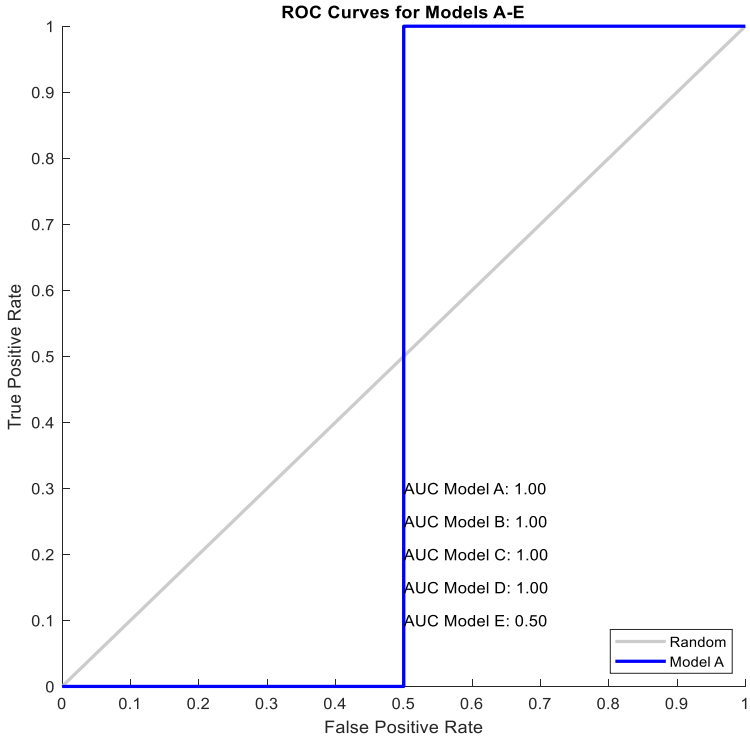

Fig. 11 Five ROC curves for models A–E obtained using the XGBoost technique

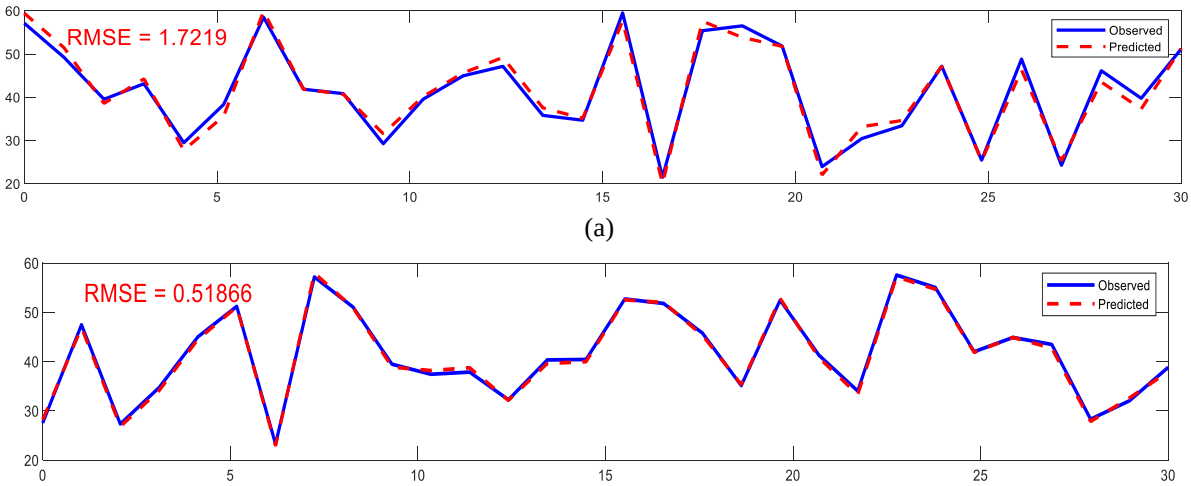

(a)

(b)

Fig. 12 RMSE plot for CNN (a), ANN-XGBoost (b)

metric, which represents the area under the ROC curve. The ROC curves that ensued were graphed, with the diagonal line serving as a representation of a classifier that operated randomly. The plotted curves depict the relationship between True Positive Rate (TPR) and False Positive Rate (FPR) for every model, demonstrating the trade-off between these two metrics. A model's ability to distinguish between positive and negative classes is typically evaluated using the Area Under the Curve (AUC) metric. A higher AUC value is generally indicative of better performance in this regard. The graphical representation exhibits the nomenclature of the models, while the Area Under the Curve (AUC) metrics are visually depicted. The presented visualization facilitates a precise comparison of model performance with respect to their capacity to accurately classify the target variable. The method enables a quantitative evaluation of the discriminative power of different models and facilitates the identification of the optimal model for the given task through visual analysis.

Fig. 12 displays the RMSE curves of two models. The x-axis denotes the data number, while the y-axis represents the predicted values. The graph displays a comparative analysis between the anticipated outcomes generated by two distinct models, namely ANN-XGBoost and CNN. The initial model, namely the Artificial Neural Network (ANN) combined with the Extreme Gradient Boosting (XGBoost)

algorithm, exhibits a Root Mean Squared Error (RMSE) of 0.518. This implies that the mean of the residuals, which represent the discrepancy between the predicted and actual values for each data point, is approximately 0.518 units. A model's predictive performance is considered to be better when its Root Mean Square Error (RMSE) is lower. The second model, Convolutional Neural Network (CNN), exhibits a Root Mean Squared Error (RMSE) of 1.721. The data indicates that the CNN model's forecasts exhibit an average deviation of roughly 1.721 units from the factual values. A higher Root Mean Square Error (RMSE) value is indicative of lower accuracy or higher prediction errors. Through a comparison of the root mean squared error (RMSE) values obtained from the two models, it was determined that the artificial neural network (ANN) boosted with extreme gradient boosting (XGBoost) outperforms the convolutional neural network (CNN) model in terms of accuracy. The ANN-XGBoost model exhibits lower prediction errors and higher accuracy in its predictions compared to the CNN model.

4. Conclusions

This research employed non-invasive features that were readily available to develop two models for the purpose of screening the likelihood of developing gastric cancer. The performance of the ANN-XGBoost model was found to be satisfactory and it has the potential to aid clinicians in screening for gastric cancer risk, in accordance with the health referral system and hierarchical levels of healthcare services. This could lead to a significant improvement in the early screening of gastric cancer on a large scale. Machine learning models have the potential to accurately identify patients at high risk for gastric cancer at an early stage. This has the potential to capture the attention of both clinicians and patients, leading to the implementation of appropriate and timely interventions aimed at improving the patients' chances of survival and quality of life. This study has the potential to assist clinical researchers in selecting and implementing the most effective prediction models, as well as assessing the primary influential factors. The findings of our study, which involved a sample of 300 patients diagnosed with gastric cancer (GC), indicate statistically significant correlations between high-risk behaviors, age at diagnosis, distant metastasis, tumor stage, and patient survival. By employing convolutional neural networks (CNN) and artificial neural networks (ANN)-eXtreme Gradient Boosting (XGBoost), we have obtained a robust predictive performance with an area under the curve (AUC) of 0.92, sensitivity of 81.5%, specificity of 90.5%, and accuracy of 84.7% in the analysis of stomach images. The results emphasize the practical significance of the identified variables and emphasize the potential of sophisticated machine learning algorithms in enhancing prognostic forecasts and directing individualized treatment approaches for patients with gastric cancer. Future research in this field would benefit from conducting further validation on larger cohorts and taking into account additional prognostic factors. Early detection and successful treatment of gastric cancer (GC) requires a thorough understanding of patient groups at higher risk, as well as reliable endoscopic diagnosis and accurate assessment of the chronically inflamed stomach. It is recommended to conduct a thorough examination of the mucosal tissue in high-risk patients using a combination of high-definition imaging techniques. The management of gastric neoplasia should be carried out by specialized referral centers that possess advanced knowledge and skills in enhanced imaging endoscopy and endoscopic resection, particularly for the treatment of early-stage cancers. Future studies should focus on validating the findings of this study on larger cohorts to enhance the generalizability of the results. Additionally, incorporating additional prognostic factors, such as molecular markers or genetic profiles, may provide deeper insights into patient outcomes and enable more accurate risk stratification. Furthermore, longitudinal studies can help assess the long-term effectiveness of the implemented machine learning models in predicting gastric cancer risk and patient survival.

Acknowledgment

Wenzhou City Public Welfare Science and Technology Project (ZY2019005). Zhejiang Provincial Natural Science Foundation of China under Grant No. LGF21H040001. The authors present their appreciation to King Saud University for funding this research through Researchers Supporting Program number (RSPD2023R704), King Saud University, Riyadh, Saudi Arabia.

The authors present their appreciation to King Saud University for funding this research through Researchers Supporting Program number (RSPD2023R704), King Saud University, Riyadh, Saudi Arabia.

References

Abdelhafiz, D., C. Yang, R. Ammar and S. Nabavi (2019), "Deep convolutional neural networks for mammography: advances, challenges and applications", *BMC Bioinform.*, **20**(11), 281 http://doi.org/10.1186/s12859-019-2823-4.

Aghakhani, M., M. Suhatril, M. Mohammadhassani, M. Daie and A. Toghroli (2015), "A simple modification of homotopy perturbation method for the solution of Blasius equation in semi-infinite domains", *Math. Probl. Eng.*, **343**, 100-126. https://doi.org/10.1155/2015/671527.

Ali, Z., Y. Deng and C. Ma (2012), "Progress of research in gastric cancer", *J. Nanosci. Nanotechnol.*, **12**(11), 8241-8248. https://doi.org/10.1166/jnn.2012.6692.

Bisschops, R., M. Areia, E. Coron, D. Dobru, B. Kaskas, R. Kuvaev, O. Pech, K. Ragunath, B. Weusten and P. Familiari (2016), "Performance measures for upper gastrointestinal endoscopy: a European Society of Gastrointestinal Endoscopy (ESGE) quality improvement initiative", *Endoscopy*, **48**(9), 843-864. http://doi.org/10.1055/s-0042-113128.

Brinker, T.J., A. Hekler, A.H. Enk and C. von Kalle (2019), "Enhanced classifier training to improve precision of a convolutional neural network to identify images of skin lesions", *PloS one*, **14**(6), e0218713 https://doi.org/10.1371/journal.pone.0218713.

Chartrand, G., P.M. Cheng, E. Vorontsov, M. Drozdzal, S. Turcotte, C.J. Pal, S. Kadoury and A. Tang (2017), "Deep learning: a primer for radiologists", *Radiographics*, **37**(7), 2113-2131. https://doi.org/10.1148/rg.2017170077

Chen, T. and C. Guestrin (2016), "Xgboost: A scalable tree boosting system", *Proceedings of the 22nd Acm Sigkdd International Conference on Knowledge Discovery and Data Mining*.

Choi, K.S., J.K. Jun, E.C. Park, S. Park, K.W. Jung, M.A. Han, I.J. Choi and H.Y. Lee (2012), "Performance of different gastric cancer screening methods in Korea: a population-based study", *PLoS One*, **7**(11), e50041.

Choi, S., S. Han, M. Roh and J. Lee (2007), "Predictive significance of serum IL-6, VEGF, and CRP in gastric adenoma and mucosal carcinoma before endoscopic submucosal dissection", *Korean J. Gastroenterol*., **1598**(9992), 2233-6869.

Conti, C.B., S. Agnesi, M. Scaravaglio, P. Masseria, M.E. Dinelli, M. Oldani and F. Uggeri (2023), "Early gastric cancer: update on prevention, diagnosis and treatment", *Int. J. Environ. Res. Publ. Health*, **20**(3), 2149. https://doi.org/10.3390/ijerph20032149

Dang, W., Xiang, L., Liu, S., Yang, B., Liu, M., Yin, Z. and Yin, L. and Zheng, W. (2023), "A feature matching method based on the convolutional neural network", *J. Imag. Sci. Technol*., **67**(3). https://doi.org/10.2352/J.ImagingSci.Technol.2023.67.3.030402

Das, N., M. Topalovic and W. Janssens (2018), "Artificial intelligence in diagnosis of obstructive lung disease: current status and future potential", *Curr. Opin. Pulm. Med*., **24**(2), 117-123. https://doi.org/10.1097/MCP.0000000000000459

Delen, D., G. Walker and A. Kadam (2005), "Predicting breast cancer survivability: A comparison of three data mining methods", *Artif. Intell. Med*., **34**(2), 113-127 https://doi.org/10.1016/j.artmed.2004.07.002.

Esteva, A., B. Kuprel, R.A. Novoa, J. Ko, S.M. Swetter, H.M. Blau and S. Thrun (2017), "Dermatologist-level classification of skin cancer with deep neural networks", *Nature*, **542**(7639), 115-118. http://doi.org/10.1038/nature21056.

Ezoe, Y., M. Muto, N. Uedo, H. Doyama, K. Yao, I. Oda, K. Kaneko, Y. Kawahara, C. Yokoi, Y. Sugiura, H. Ishikawa, Y. Takeuchi, Y. Kaneko and Y. Saito (2011), "Magnifying narrowband imaging is more accurate than conventional white-light imaging in diagnosis of gastric mucosal cancer", *Gastroenterology*, **141**(6), 2017-2025.e2013 https://doi.org/10.1053/j.gastro.2011.08.007.

Fujishiro, M., S. Yoshida, R. Matsuda, A. Narita, H. Yamashita and Y. Seto (2017), "Updated evidence on endoscopic resection of early gastric cancer from Japan", *Gastr. Cancer*, **20**(1), 39-44. http://doi.org/10.1007/s10120-016-0647-8.

He, B., Zhang, Y., Zhou, Z., Wang, B., Liang, Y., Lang, J., Lin, H., Bing, P., Yu, L., Sun, D., Luo, H, Yang, J. and Tian, G. (2020), "A neural network framework for predicting the tissue-of-origin of 15 common cancer types based on RNA-seq data", *Front. Bioeng. Biotechnol*., **8**, 737. https://doi.org/10.3389/fbioe.2020.00737

Hirasawa, T., K. Aoyama, T. Tanimoto, S. Ishihara, S. Shichijo, T. Ozawa, T. Ohnishi, M. Fujishiro, K. Matsuo, J. Fujisaki and T. Tada (2018), "Application of artificial intelligence using a convolutional neural network for detecting gastric cancer in endoscopic images", *Gastr. Cancer*, **21**(4), 653-660. http://doi.org/10.1007/s10120-018-0793-2.

Horie, Y., T. Yoshio, K. Aoyama, S. Yoshimizu, Y. Horiuchi, A. Ishiyama, T. Hirasawa, T. Tsuchida, T. Ozawa, S. Ishihara, Y. Kumagai, M. Fujishiro, I. Maetani, J. Fujisaki and T. Tada (2019), "Diagnostic outcomes of esophageal cancer by artificial intelligence using convolutional neural networks", *Gastrointest. Endosc*., **89**(1), 25-32. https://doi.org/10.1016/j.gie.2018.07.037.

Huang, Y., J. Xu, Y. Zhou, T. Tong, X. Zhuang and A.S.D.N. Initiative (2019), "Diagnosis of Alzheimer's disease via multi-modality 3D convolutional neural network", *Front. Neurosci*., **13**, 509. https://doi.org/10.3389/fnins.2019.00509.

Jagerman, R., X. Wang, H. Zhuang, Z. Qin, M. Bendersky and M. Najork (2022), "Rax: Composable learning-to-rank using JAX", *Proceedings of the 28th ACM SIGKDD Conference on Knowledge Discovery and Data Mining*, Washington D.C., U.S.A., August.

Kadowaki, S., K. Tanaka, H. Toyoda, R. Kosaka, I. Imoto, Y. Hamada, M. Katsurahara, H. Inoue, M. Aoki and T. Noda (2009), "Ease of early gastric cancer demarcation recognition: a comparison of four magnifying endoscopy methods", *J. Gastroenterol. Hepatol*., **24**(10), 1625-1630. https://doi.org/10.1111/j.1440-1746.2009.05918.x.

Kaise, M., M. Kato, M. Urashima, Y. Arai, H. Kaneyama, Y. Kanzazawa, J. Yonezawa, Y. Yoshida, N. Yoshimura and T. Yamasaki (2009), "Magnifying endoscopy combined with narrow-band imaging for differential diagnosis of superficial depressed gastric lesions", *Endoscopy*, **41**(4), 310-315. http://doi.org/10.1055/s-0028-1119639.

Kalan Farmanfarma, K., N. Mahdavifar, S. Hassanipour and H. Salehiniya (2020), "Epidemiologic study of gastric cancer in iran: a systematic review", *Clin. Experim. Gastroenterol*. **13**, 511-542. http://doi.org/10.2147/CEG.S256627.

Kim, Y.S. (2008), "Comparison of the decision tree, artificial neural network, and linear regression methods based on the number and types of independent variables and sample size", *Expert Syst. Appl*., **34**(2), 1227-1234. https://doi.org/10.1016/j.eswa.2006.12.017.

Kim, Y.S. (2010), "Performance evaluation for classification methods: A comparative simulation study", *Expert Syst. Appl*., **37**(3), 2292-2306. https://doi.org/10.1016/j.eswa.2009.07.043.

Li, B., S. Ding, G. Song, J. Li and Q. Zhang (2019), "Computer-aided diagnosis and clinical trials of cardiovascular diseases based on artificial intelligence technologies for risk-early warning model", *J. Med. Syst*., **43**(7), 228. http://doi.org/10.1007/s10916-019-1346-x.

Liang, Y., W. Wang, C. Fang, S.S. Raj, W.M. Hu, Q. W. Li and Z. W. Zhou (2016), "Clinical significance and diagnostic value of serum CEA, CA19-9 and CA72-4 in patients with gastric cancer", *Oncotarget*, **7**(31), 49565-49573 http://doi.org/10.18632/oncotarget.10391.

Lu, S., Yang, B., Xiao, Y., Liu, S., Liu, M., Yin, L. and Zheng, W. (2023), "Iterative reconstruction of low-dose CT based on differential sparse", *Biomed. Signal Pr. Control*, **79**, 104204. https://doi.org/10.1016/j.bspc.2022.104204

Lu, S., Yang, J., Yang, B., Yin, Z., Liu, M., Yin, L. and Zheng, W. (2023), "Analysis and design of surgical instrument localization algorithm", *Comput. Model. Eng. Sci*., **137**(1), 669-685. https://doi.org/10.32604/cmes.2023.027417

Mahmoodi, S.A., K. Mirzaie and S.M. Mahmoudi (2016), "A new algorithm to extract hidden rules of gastric cancer data based on ontology", *SpringerPlus*, **5**(1), 312. http://doi.org/10.1186/s40064-016-1943-9.

Mansouri, I., M. Safa, Z. Ibrahim, O. Kisi, M.M. Tahir, S. Baharom and M. Azimi (2016), "Strength prediction of rotary brace damper using MLR and MARS", *Struct. Eng. Mech*. **60**(3), 471-488. http://doi.org/10.12989/sem.2016.60.3.471.

Mohammadhassani, M., A.M.D. Saleh, M. Suhatril and M. Safa (2015), "Fuzzy modelling approach for shear strength prediction of RC deep beams", *Smart Struct. Syst*., **16**(3), 497-519. https://doi.org/10.12989/sss.2015.16.3.497.

Muto, M., K. Yao, M. Kaise, M. Kato, N. Uedo, K. Yagi and H. Tajiri (2016), "Magnifying endoscopy simple diagnostic algorithm for early gastric cancer (MESDA-G)", *Digest. Endosc*., **28**(4), 379-393. https://doi.org/10.1111/den.12638.

Pimentel-Nunes, P., M. Dinis-Ribeiro, J. Soares, R. Marcos-Pinto, C. Santos, C. Rolanda, R. Bastos, M. Areia, L. Afonso and J. Bergman (2012), "A multicenter validation of an endoscopic classification with narrow band imaging for gastric pre-

cancerous and cancerous lesions", *Endoscopy*, **44**(03), 236-246. http://doi.org/10.1055/s-0031-1291537.

Safa, M., M. Ahmadi, J. Mehrmashadi, D. Petkovic, M. Mohammadhassani, Y. Zandi and Y. Sedghi (2020), "Selection of the most influential parameters on vectorial crystal growth of highly oriented vertically aligned carbon nanotubes by adaptive neuro-fuzzy technique", *Int. J. Hydromechatr.*, **3**(3), 238-251. https://doi.org/10.1504/IJHM.2020.109919.

Sari, P.A., M. Suhatril, N. Osman, M.A. Mu'azu, H. Dehghani, Y. Sedghi, M. Safa, M. Hasanipanah, K. Wakil and M. Khorami (2019), "An intelligent based-model role to simulate the factor of safe slope by support vector regression", *Eng. Comput.*, **35**(4), 1521-1531. https://doi.org/10.1007/s00366-018-0677-4.

Shibagaki, K., Y. Amano, N. Ishimura, H. Taniguchi, H. Fujita, S. Adachi, E. Kakehi, R. Fujita, K. Kobayashi and Y. Kinoshita (2015), "Diagnostic accuracy of magnification endoscopy with acetic acid enhancement and narrow-band imaging in gastric mucosal neoplasms", *Endoscopy*, 16-25. https://doi.org/10.1055/s-0034-1392542

Shibata, T., A. Teramoto, H. Yamada, N. Ohmiya, K. Saito and H. Fujita (2020), "Automated detection and segmentation of early gastric cancer from endoscopic images using mask R-CNN", *Appl. Sci.*, **10**(11), 3842. https://doi.org/10.3390/app10113842.

Shichijo, S., S. Nomura, K. Aoyama, Y. Nishikawa, M. Miura, T. Shinagawa, H. Takiyama, T. Tanimoto, S. Ishihara, K. Matsuo and T. Tada (2017), "Application of convolutional neural networks in the diagnosis of helicobacter pylori infection based on endoscopic images", *EBioMedicine*, **25**, 106-111. https://doi.org/10.1016/j.ebiom.2017.10.014.

Shitrit, D., B. Zingerman, A.B.G. Shitrit, D. Shlomi and M.R. Kramer (2005), "Diagnostic value of CYFRA 21-1, CEA, CA 19-9, CA 15-3, and CA 125 assays in pleural effusions: analysis of 116 cases and review of the literature", *The Oncologist*, **10**(7), 501-507. http://doi.org/10.1634/theoncologist.10-7-501.

Song, X., Li, Q. and Zhang, J. (2023), "A double-edged sword: DLG5 in diseases", *Biomed. Pharmacother.*, **162**, 114611. https://doi.org/10.1016/j.biopha.2023.114611

Taninaga, J., Y. Nishiyama, K. Fujibayashi, T. Gunji, N. Sasabe, K. Iijima and T. Naito (2019), "Prediction of future gastric cancer risk using a machine learning algorithm and comprehensive medical check-up data: A case-control study", *Sci. Rep.*, **9**(1), 12384. http://doi.org/10.1038/s41598-019-48769-y.

Toghroli, A., E. Darvishmoghaddam, Y. Zandi, M. Parvan, M. Safa, M.M. Abdullahi, A. Heydari, K. Wakil, S.A.M. Gebreel and M. Khorami (2018), "Evaluation of the parameters affecting the Schmidt rebound hammer reading using ANFIS method", *Comput. Concr.*, **21**(5), 525-530. http://doi.org/10.12989/cac.2018.21.5.525.

Ture, M., F. Tokatli and I. Kurt Omurlu (2009), "The comparisons of prognostic indexes using data mining techniques and Cox regression analysis in the breast cancer data", *Exp. Syst. Appl.*, **36**(4), 8247-8254. https://doi.org/10.1016/j.eswa.2008.10.014.

Watanabe, Y., H.S. Kim, R.J. Castoro, W. Chung, M.R.H. Estecio, K. Kondo, Y. Guo, S.S. Ahmed, M. Toyota, F. Itoh, K.T. Suk, M.Y. Cho, L. Shen, J. Jelinek and J.P.J. Issa (2009), "Sensitive and specific detection of early gastric cancer with DNA methylation analysis of gastric washes", *Gastroenterology*, **136**(7), 2149-2158. https://doi.org/10.1053/j.gastro.2009.02.085.

White, J.R., S.S. Sami, D. Reddiar, J. Mannath, J. Ortiz-Fernández-Sordo, S. Beg, R. Scott, P. Thiagarajan, S. Ahmad, A. Parra-Blanco, M. Kasi, E. Telakis, A.A. Sultan, J. Davis, A. Figgins, P. Kaye, K. Robinson, J.C. Atherton and K. Ragunath (2018), "Narrow band imaging and serology in the assessment of premalignant gastric pathology", *Scand. J. Gastroenterol.*, **53**(12), 1611-1618. http://doi.org/10.1080/00365521.2018.1542455.

Wu, J., G. Li, Z. Wang, Y. Yao, R. Chen, X. Pu and J. Wang (2015), "Circulating MicroRNA-21 is a potential diagnostic biomarker in gastric cancer", *Disease Markers*, 435656. http://doi.org/10.1155/2015/435656.

Yamaguchi, Y., Y. Nagata, R. Hiratsuka, Y. Kawase, T. Tominaga, S. Takeuchi, S. Sakagami and S. Ishida (2016), "Gastric cancer screening by combined assay for serum anti-Helicobacter pylori IgG antibody and serum pepsinogen levels-the ABC method", *Digestion*, **93**(1), 13-18. https://doi.org/10.1159/000441742.

Yao, K. (2015), "Clinical application of magnifying endoscopy with narrow-band imaging in the stomach", *Clin. Endosc.*, **48**(6), 481-490. http://doi.org/10.5946/ce.2015.48.6.481.

Zhang, Q., Z.Y. Chen, C.D. Chen, T. Liu, X.W. Tang, Y.T. Ren, S.L. Huang, X.B. Cui, S.L. An, B. Xiao, Y. Bai, S.D. Liu, B. Jiang, F.C. Zhi and W. Gong (2015), "Training in early gastric cancer diagnosis improves the detection rate of early gastric cancer: an observational study in China", *Medicine (Baltimore)*, **94**(2), e384. http://doi.org/10.1097/md. 384.

Zhou, B., Z. Zhou, Y. Chen, H. Deng, Y. Cai, X. Rao, Y. Yin and L. Rong (2020), "Plasma proteomics-based identification of novel biomarkers in early gastric cancer", *Clin. Biochem.*, **76**, 5-10. https://doi.org/10.1016/j.clinbiochem.2019.11.001.

Zhu, Y., Huang, R., Wu, Z., Song, S., Cheng, L. and Zhu, R. (2021), "Deep learning-based predictive identification of neural stem cell differentiation", *Nature Commun.*, **12**(1), 2614. https://doi.org/10.1038/s41467-021-22758-0

Zhu, Y., S. Ge, L. Zhang, X. Wang, X. Xing, Y. Hu, Y. Li, Y. Jia, Y. Lin and B. Fan (2012), "Clinical value of serum CEA, CA19-9, CA72-4 and CA242 in the diagnosis and prognosis of gastric cancer", *Chinese J. Gastrointest. Surg.*, **15**(2), 161-164.

Zhuang, Y., Chen, S., Jiang, N. and Hu, H. (2022), "An effective wssenet-based similarity retrieval method of large lung CT image databases", *KSII Transact. Internet Inform. Syst.*, **16**(7). https://doi.org/10.3837/tiis.2022.07.013

CC